Aldosteronism: an immunostimulatory state precedes proinflammatory/fibrogenic cardiac phenotype

Ivan C. Gerling,[1] Yao Sun,[2] Robert A. Ahokas,[3] Linus A. Wodi,[2] Syamal K. Bhattacharya,[4] Kenneth J. Warrington,[5] Arnold E. Postlethwaite,[5] and Karl T. Weber[2]
Divisions of [1]Endocrinology, [2]Cardiovascular Diseases, and [5]Connective Tissue Diseases,
Department of Medicine; and Departments of [3]Obstetrics and Gynecology and [4]Surgery,
University of Tennessee Health Science Center, Memphis, Tennessee 38163

Gerling, Ivan C., Yao Sun, Robert A. Ahokas, Linus A. Wodi, Syamal K. Bhattacharya, Kenneth J. Warrington, Arnold E. Postlethwaite, and Karl T. Weber. Aldosteronism: an immunostimulatory state precedes proinflammatory/fibrogenic cardiac phenotype. *Am J Physiol Heart Circ Physiol* 285: H813–H821, 2003; 10.1152/ajpheart.00113.2003.—Chronic inappropriate (relative to dietary Na^+ intake) elevations in circulating aldosterone (ALDO), termed aldosteronism, are associated with remodeling of intramural arteries of the right and left heart. Lesions appear at *week 4* of treatment with ALDO and 1% dietary NaCl in uninephrectomized rats (ALDOST) and include invading monocytes, macrophages and lymphocytes with intracellular evidence of oxidative and nitrosative stress, myofibroblasts, and perivascular fibrosis. In this study, we tested the hypothesis that an immunostimulatory state with activated circulating peripheral blood mononuclear cells (PBMCs) precedes this proinflammatory and profibrogenic cardiac phenotype and is initiated by reduction in the cytosolic free Mg^{2+} concentration ($[Mg^{2+}]_i$). At 1 and 4 wk of ALDOST (preclinical and clinical stages, respectively), we monitored serum Mg^{2+}, PBMC $[Mg^{2+}]_i$ and cytosolic free $[Ca^{2+}]$ (via fluorimetry), and expressed genes (via microchip array) as well as markers of oxidative and nitrosative stress in plasma [α_1-antiproteinase activity (α_1-AP)] and cardiac tissue (immunohistochemical detection of $gp91^{phox}$ subunit of NADPH oxidase and 3-nitrotyrosine). Age- and gender-matched unoperated and untreated (UO) rats and uninephrectomized salt-treated (UN) rats served as controls. Serum $[Mg^{2+}]$ was unchanged by ALDOST. In contrast with UO and UN, $[Mg^{2+}]_i$ and plasma α_1-AP were each reduced ($P < 0.05$) at *weeks 1* and *4*. The decline in PBMC $[Mg^{2+}]_i$ was accompanied by Ca^{2+} loading. Differential (twofold and higher) expression (up- and downregulation) in PBMC transcriptomes was present at *week 1* and progressed at *week 4*. Involved were genes for the α_1-isoform of Na^+-K^+-ATPase, the ATP-dependent Ca^{2+} pump, antioxidant reserves, inducible nitric oxide synthase, and PBMC activation with autoimmune responses. Expression of 3-nitrotyrosine and activation of $gp91^{phox}$ were seen in inflammatory cells that invaded intramural arteries. Thus early in aldosteronism (preclinical stage), an immunostimulatory state featuring activated circulating PBMCs with reduced ionized $[Mg^{2+}]_i$ and oxidative and nitrosative stress precedes and may even predispose to coronary vascular lesions that first appear at *week 4*.

peripheral blood mononuclear cells; ionized magnesium; oxidative and nitrosative stress; transcriptome; pathology

---

IN BOTH HUMANS AND RATS and whether derived from endogenous or exogenous sources, chronic inappropriate (relative to dietary Na^+ intake) elevations in circulating aldosterone (ALDO) are associated with structural remodeling of intramural arteries of the right and left heart and systemic organs (9, 14, 15, 27, 39, 45, 52, 53, 63, 66, 75). Coronary vascular lesions in uninephrectomized rats first appear at 4 wk of ALDO-and-salt treatment (ALDOST) and involve progressively more vascular sites with continued treatment (64). Lesions consist of circulating monocytes, macrophages and lymphocytes that have invaded the perivascular space; fibroblastlike cells or myofibroblasts that express fibrillar type I and III collagens; and ultimately a perivascular fibrosis (15, 27, 39, 45, 52, 53, 64). Sun et al. (65) addressed cellular and molecular events that are involved in the appearance of this proinflammatory and profibrogenic cardiac phenotype. When studied using immunohistochemistry, oxidative and nitrosative stress appeared within inflammatory cells that had invaded the coronary vasculature together with activation of the redox-sensitive nuclear transcription factor NF-κB and upregulated mRNA expression of a proinflammatory mediator cascade that it regulates that includes intercellular adhesion molecule (ICAM)-1, monocyte chemoattractant protein (MCP)-1, and tumor necrosis factor (TNF)-α. Such neurohormonal activation occurs in chronic cardiac failure and is accompanied by increased expression of TNF-family ligands and oxidative stress in peripheral blood mononuclear cells (PBMCs; Refs. 18, 74). The mechanisms that are responsible for the induction of oxidative and nitrosative stress and activation of PBMCs in aldosteronism are unclear.

Mg^{2+} is involved in myriad reactions and functions in various cells including PBMCs. These include enzymatic reactions, operation of channels, receptors, and intracellular signaling molecules, and conformation of

---

nucleic acids and proteins (22, 50, 54, 55). ALDO influences Mg^{2+} homeostasis, including increased urinary Mg^{2+} excretion and reduced PBMC ionized Mg^{2+} levels (20, 30). In this study, we investigated the hypothesis that an immunostimulatory state with activated circulating PBMCs precedes the proinflammatory and profibrogenic cardiac phenotype in aldosteronism and is induced by a reduction in the cytosolic Mg^{2+} concentration ($[Mg^{2+}]_i$). Toward this end, we monitored the PBMC transcriptome or the genes that it expresses together with markers of oxidative and nitrosative stress in plasma and invading inflammatory cells, and levels of PBMC $[Mg^{2+}]_i$ and cytosolic Ca^{2+} concentration ($[Ca^{2+}]_i$) at 1 and 4 wk of ALDOST; these represent the preclinical and clinical stages of aldosteronism, respectively.

MATERIALS AND METHODS

Animals. Eight-week-old male Sprague-Dawley rats (Harlan) were used. The study was approved by the institution's Animal Care and Use Committee. Unoperated and untreated (UO) age-matched rats served as one control group ($n = 5$). Uninephrectomized rats that received 1% NaCl/0.4% KCl in drinking water and standard laboratory feed served as a second control group ($n = 10$). Separate groups of uninephrectomized salt-treated (UN) rats received ALDO (0.75 μg/h) via implanted minipump for 1 or 4 wk ($n = 10$ at each time point). This dose of ALDO promptly raises plasma levels to those seen in humans with congestive heart failure or primary aldosteronism (PAL); it also rapidly suppresses plasma renin activity and circulating angiotensin II levels (9, 24). Animals were observed daily to monitor physical activity and food and water consumption. Systolic blood pressure was recorded as previously reported (65). At the conclusion of *wk 1* or *4* of ALDOST, animals were weighed and anesthetized, blood was obtained by cardiac puncture, and hearts were harvested.

Plasma Mg^{2+} concentrations. Total Mg^{2+} concentrations in 1:20-fold diluted plasma were determined in 100-μl specimens using a Varian model 220 FS double-beam fast sequential atomic absorption spectrophotometer (Varian Techtron; Melbourne, Australia) and were expressed in milligrams per deciliter (5).

$[Mg^{2+}]_i$ and $[Ca^{2+}]_i$ in PBMCs. A modification of the method of Delva et al. (20) was used for the isolation of PBMCs and the measurement of $[Mg^{2+}]_i$ and $[Ca^{2+}]_i$. Briefly, PBMCs were isolated by Histopaque 1083 centrifugation for 30 min at 400 g. Cells were carefully aspirated, washed twice, suspended in PBS, and counted with a hemocytometer.

For the measurement of $[Mg^{2+}]_i$, three separate aliquots of PBMCs (1×10^6 cells each) were suspended in RPMI 1640 and 0.1% BSA (vol/vol) with the cell-permeant dye mag-fura 2-acetoxymethyl ester (mag-fura 2-AM, 10 μmol/l; Molecular Probes; Eugene, OR) and incubated for 1 h at 37°C. After centrifugation, cells were washed twice with RPMI 1640 and 0.1% BSA for removal of extracellular dye and were resuspended in the same medium. Cells were incubated for an additional 45 min at room temperature to allow complete deesterification of the intracellular dye. The cells were then centrifuged and suspended in 2 ml of buffer [that contained (in mmol/l) 140 NaCl, 5 KCl, 1.8 CaCl₂, 0.8 MgSO₄, 15 HEPES, and 5 D-glucose (pH 7.4)], transferred to a quartz cuvette, and measured fluorimetrically using a spectrofluorometer (model LS-50B, Perkin-Elmer). Fluorescence emission at 510 nm (slit width, 5 nm) was measured at alternate

excitations of 335 and 370 nm (slit width, 10 nm). After initial fluorescence was measured, 5 mmol/l each of EDTA and EGTA were added to the cuvette to chelate extracellular Mg^{2+}, and fluorescence values at 335 and 370 nm were read again for calculation of the free resting $[Mg^{2+}]_i$ ratio (R). Triton X-100 was then added at a final concentration of 0.1% to lyse the cells, and fluorescence values at 335 and 370 nm were read again for calculation of the minimum fluorescence ratio (R_{min}). Subsequently $MgSO_4$ (100 mmol/l) was added to the cuvette, and the fluorescence values at 335 and 370 nm were read for calculation of the maximum fluorescence ratio (R_{max}). $[Mg^{2+}]_i$ was then calculated as follows: $[Mg^{2+}]_i = K_d \times [(R - R_{min})S\mu] \div [(R_{max} - R)Sb]$, where K_d for the Mg^{2+}-mag-fura 2 complex is 1.5 mmol/l (49), R is the free resting fluorescence ratio at 335:370 after addition of EDTA and EGTA, R_{min} is the fluorescence ratio at 335:370 after cell lysis with Triton X-100, R_{max} is the fluorescence ratio at 335:370 after addition of $MgSO_4$, and $S\mu$ and Sb are the fluorescence intensities at 370 nm with zero Mg^{2+} and excess Mg^{2+}, respectively.

The $[Ca^{2+}]_i$ of PBMCs was measured with the fluorescent dye fura 2-AM. Three separate aliquots of cells (1×10^6 cells each) were incubated in RPMI 1640 medium with fura 2-AM dye (5 μmol/l) for 30 min at 37°C. The cells were centrifuged, washed to remove extracellular dye, and incubated in the same medium for 45 min at room temperature as for the $[Mg^{2+}]_i$ assay. For the fluorimetric $[Ca^{2+}]_i$ measurements, cells were suspended in the same buffer for $[Mg^{2+}]_i$ as described above but without $CaCl_2$. Fluorescence emission values at 510 nm (slit width, 10 nm) with alternating excitations at 340 and 380 nm (slit width, 10 nm) were read at baseline, after addition of EGTA (10 mmol/l) to chelate Ca^{2+}, after addition of Triton X-100 to lyse the cells, and after addition of excess Ca^{2+} (10 mmol/l $CaCl_2$). $[Ca^{2+}]_i$ was calculated with the same equation as that for Mg^{2+}, where K_d for the Ca^{2+}-fura 2 complex was 225 nmol/l (26).

Measurement of plasma α_1-antiproteinase. Reactive oxygen and nitrogen species generated from oxidative stress inactivate α_1-antiproteinase (α_1-AP) by oxidizing an essential methionine at positions 1, 8, or 358 of the active-site loop to methionine sulfoxide (8). Thus the measurement of active α_1-AP in body fluids is a biomarker used to assess the presence of oxidative and nitrosative stress (19, 25, 46). Plasma concentrations of α_1-AP were measured using a commercially available kit (Oxis Research; Portland, OR). Briefly, plasma was diluted 1:50 with Tris·HCl-phosphate buffer (pH 8.0). Diluted plasma (50 μl) or assay buffer (for controls) was added to a test tube that contained buffer (500 μl) and 2 μM elastase (50 μl) in assay buffer. The tubes were incubated at 37°C for 5 min and subsequently incubated at room temperature for 5 min. This method is based on the measurement of elastase activity and cleavage of N-succinyl-(Ala)3-p-nitroanilide (NASAN), which results in the production of the chromagen p-nitroaniline. Thus the substrate solution NASAN (400 μl) was added to the tube, mixed by vortexing, and immediately transferred to a cuvette. Absorbance values at 410 nm were recorded for at least 1 min to determine the rate of change in absorbance from the slope of the line vs. time (ΔA_{410}). The concentration of α_1-AP (in μM) was then calculated as follows: α_1-AP = (ΔA_{410} control $- \Delta A_{410}$ sample $\div \Delta A_{410}$ control) $\times 2d$, where d is the dilution factor of the plasma sample before addition to the assay tube, and the factor 2 represents the elastase concentration (in μM). Because α_1-AP is an irreversible equimolar inhibitor of elastase, the concentration of active α_1-AP in a sample is equivalent to the concentration of elastase that

is inhibited. The intra- and interassay percent coefficients of variability for this assay were ≤6%. The detection limit for this assay was 0.5 µM.

PBMC transcriptomes. Total RNA was isolated from purified PBMCs using a tri-reagent (TRIzol, Invitrogen; Carlsbad, CA). Gene-expression analysis was conducted on the Affymetrix rat genome U34A chip (Affymetrix; San Diego, CA) probing ~7,000 known genes and 1,000 expressed sequence tags (EST). The gene-expression analysis was conducted by a company that provides this core service for our institution on contract. Detailed protocols and descriptions of analyses are available on their web site (http://www.genome-explorations.com). Briefly, the quality of total RNA was ensured by analysis using an Agilent Bioanalyzer 2100 "Lab on a Chip" system. RNA was then used to synthesize first- and second-strand cDNA. Double-stranded cDNA was used in an in vitro transcription step to synthesize biotin-labeled cRNA. Transcript quality was assessed again at this step by comparing the 5′-to-3′ ratios of a collection of housekeeping genes. Samples that passed both quality-control steps were hybridized to the expression-array chip and relative expression levels for each probe set (gene or EST) were collected and analyzed using Microarray Suite 5.0 software (Affymetrix). This software was used to normalize the data, evaluate the quality of the data sets, and conduct basic comparisons between data from two samples. Comparative analyses of samples produced a list of differentially expressed genes that are defined as genes with expression levels that are significantly different and at least different by a factor of $1 \times \log 2$. A total of six UO controls, six ALDOST samples obtained at 1 wk, and six ALDOST samples obtained at 4 wk went into the characterization of transcriptomes. Each sample that was analyzed on expression-array chips consisted of pooled RNA from three animals. We compared transcriptomes from untreated controls to samples obtained at *weeks 1* and *4* of ALDOST to produce a list of genes that are affected by the treatment. The experiment was repeated, and only genes that show differential expression in response to treatment in both of these independent experiments are reported in the lists of specific differentially expressed genes (see Tables 2 and 3).

Cardiac pathology. Expressions of oxidative and nitrosative stress were studied by immunohistochemical localization of gp91phox and 3-nitrotyrosine, respectively. Coronal cryostat sections (6 µm) were prepared, air dried, fixed in 10% buffered formalin for 5 min, and washed in PBS for 10 min. Sections were then incubated with primary antibody against gp91phox at a dilution of 1:100 (12) or 3-nitrotyrosine at a dilution of 1:100 (Upstate Biotech; Waltham, MA) in PBS that contained 1% BSA for 60 min. Sections were then washed in PBS for 10 min and incubated with IgG-peroxidase-conjugated secondary antibody (Sigma; St. Louis, MO) at a dilution of 1:150, washed in PBS for 10 min, incubated with 0.5 mg/ml diaminobenzidine tetrahydrochloride 2-hydrate + 0.05% H_2O_2 for 10 min, and again washed in PBS. Negative control sections were incubated with secondary antibody alone, stained with hematoxylin, dehydrated, mounted, and examined using light microscopy.

Statistical analysis. Plasma Mg^{2+}, $[Mg^{2+}]_i$, $[Ca^{2+}]_i$, and α_1-AP results are expressed as means ± SE. Data were analyzed by ANOVA, and significant differences between groups were determined using the Student-Newman-Keuls multiple-comparisons test. Differences were considered statistically significant when $P < 0.05$.

RESULTS

Animals. During *week 1* of ALDOST, animals appeared healthy: they were active, eating, drinking, and gaining body wt (200 ± 5 g, which was not different from body wt of UO and UN control groups, 198 ± 5 and 203 ± 16 g, respectively). After this preclinical stage and at *week 4* of ALDOST (clinical stage), animals were lethargic and anorectic and had gained significantly less weight (265 ± 8 g; $P < 0.05$) compared with UO and UN controls (345 ± 6 and 340 ± 17 g, respectively). We did not observe aural hyperemia, tetany, or convulsions in ALDOST animals. Systolic blood pressure at *week 1* ALDOST was no different from UO or UN controls (114 ± 11 vs. 109 ± 12 and 110 ± 7 mmHg, respectively). At *week 4*, systolic blood pressure was elevated (173 ± 21 mmHg; $P < 0.05$) compared with controls and *week 1* values.

Plasma Mg^{2+} concentrations. Plasma concentrations of Mg^{2+} at *week 1* of ALDOST (1.52 ± 0.08 mg/dl) were no different than UO controls (1.40 ± 0.06 mg/dl) and UN controls (1.54 ± 0.06 mg/dl). Plasma values for this divalent cation remained unchanged from controls at 4 wk of ALDOST (1.51 ± 0.05 mg/dl).

$[Mg^{2+}]_i$ and $[Ca^{2+}]_i$ in PBMCs. As seen in Figs. 1 and 2, values for $[Mg^{2+}]_i$ and $[Ca^{2+}]_i$ did not differ between UO and UN controls. One week of ALDOST was accompanied by a significant ($P < 0.05$) decline in $[Mg^{2+}]_i$ and $[Ca^{2+}]_i$. At *week 4* of ALDOST, $[Mg^{2+}]_i$ remained reduced compared with controls ($P < 0.05$), whereas $[Ca^{2+}]_i$ had increased ($P < 0.05$) compared with controls and *week 1* values.

Plasma α_1-AP. Plasma levels of α_1-AP correlate inversely with oxidative and nitrosative stress (19, 25, 46) and with the generation of oxygen metabolites and peroxynitrite, a product of the reaction of superoxide with nitric oxide (34). Levels of α_1-AP (Fig. 3) were no different between UO- and UN-control groups. During preclinical and clinical stages that corresponded to *wks 1* and *4* of ALDOST, plasma α_1-AP values were significantly ($P < 0.05$) reduced in keeping with an early and sustained induction of oxidative and nitrosative stress.
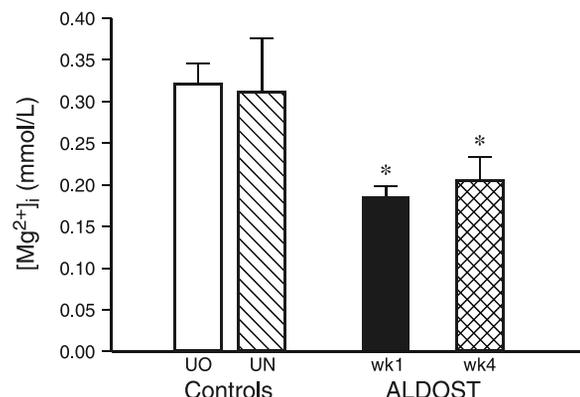

Fig. 1. Peripheral blood mononuclear cell (PBMC) free cytosolic Mg^{2+} concentrations ($[Mg^{2+}]_i$) in unoperated and untreated (UO) controls and uninephrectomized salt-treated (UN) controls are shown together with values obtained at *weeks 1* and *4* of aldosterone-and-salt treatment (ALDOST). *$P < 0.05$ vs. controls.
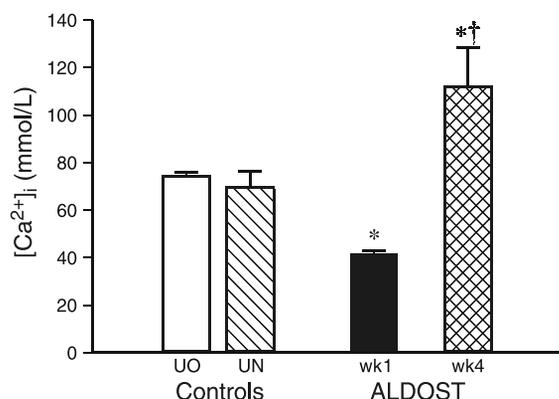
Fig. 2. PBMC free cytosolic Ca^{2+} concentrations ($[Ca^{2+}]_i$) for UO, UN, and *wks 1* and *4* ALDOST. *$P < 0.05$ vs. controls; †$P < 0.05$ vs. *wk 1*.

PBMC transcriptomes. An up- or downregulation in PBMC gene expression was progressively influenced by ALDOST. Relative to controls, we found a differential (twofold and greater) change in expression at *weeks 1* and *4* that involved 205 and 431 genes or ESTs, respectively (Table 1). A total of 564 genes or ESTs were differentially expressed at one or both times. Of the 72 genes or ESTs that were differentially expressed at *weeks 1* and *4*, 37 were increased at both times, 30 were decreased at both times (relative to controls), and 5 were differentially expressed in opposite directions at *weeks 1* and *4*. Whereas 133 of 205 genes and ESTs were uniquely expressed during the preclinical stage at *week 1*, 359 of 431 genes and ESTs were uniquely expressed at *week 4*, which suggests that new pathological processes had been initiated.

Within the lists of specific genes that are affected by ALDOST, we found a number of genes with products that are affected by or dependent on cations (Table 2). For example, the documented decrease in $[Mg^{2+}]_i$ appears to affect a downregulation of the α_1-isoform of Na^+-K^+-ATPase and the corresponding increase in intracellular Ca^{2+} to affect an upregulation of an ATP-dependent Ca^{2+} pump as well as a number of Ca^{2+}-dependent genes. Furthermore, we found an upregulation of genes that is associated with producing and
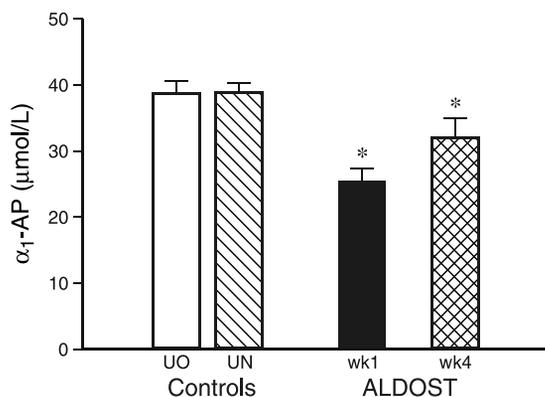

Fig. 3. Plasma α_1-antiproteinase (α_1-AP) for UO, UN, and *weeks 1* and *4* ALDOST. *$P < 0.05$ vs. controls.

Table 1. *Number of differentially expressed genes in PBMC from ALDOST compared with unoperated and untreated control rats*

| ALDOST, wk | Genes, no. expressed | | |
	Increased expression	Decreased expression	Total
1	113	92	205
4	230	201	431

PBMC, peripheral blood mononuclear cells; ALDOST, uninephrectomized rats treated with aldosterone and salt.

counteracting oxidative stress such as inducible nitric oxide synthase (iNOS) and Mn^{2+}-SOD (Table 3). Other indications of inflammatory response activation included increased expression of ICAM-1 as well as chemokines, cytokines, and the associated receptors. Finally, activation of lymphocytes and production of specific immune responses including autoimmune responses were evident (Table 3).

Cardiac pathology. Microscopic evidence of cardiac pathology involving the invasion of intramural coronary arteries of both ventricles by monocytes, macrophages, and lymphocytes was first seen at *week 4* of ALDOST. At these vascular sites (which involve right and left ventricles), immunohistochemical evidence of gp91[phox] expression (Fig. 4, *A* and *B*) and the presence of 3-nitrotyrosine (Fig. 4, *C* and *D*) was found. Cardiac morphology at *week 1* ALDOST was no different from controls.

DISCUSSION

Sun et al. (65) have shown that the proinflammatory and profibrogenic cardiac phenotype that involves intramural arteries of the right and left heart in chronic ALDOST rats is related to an induction of oxidative and nitrosative stress and is prevented by antioxidant cotreatment. In this study, we investigated the hypothesis that activation of circulating monocytes, macrophages, and lymphocytes or PBMCs (including the altered redox potential) is related to reduction in $[Mg^{2+}]_i$ composition. Our study led to several major findings.

First, a reduction in $[Mg^{2+}]_i$ occurred at *week 1* of ALDOST, which is a preclinical stage, before the appearance of systemic illness with anorexia and leth-

Table 2. *Differentially expressed genes dependent on cations in ALDOST compared with unoperated and untreated control rats*

Gene Product	Effect of ALDO	Fold Change
Na^+-K^+-ATPase α_1-isoform	Decrease	7.3
ATP-dependent RNA helicase	Decrease	2.7
cGMP-stimulated phosphodiesterase	Decrease	9.8
ATP-dependent Ca^{2+} pump	Increase	3.2
Lipocortin I (Ca^{2+} binding)	Increase	4.3
Calmodulin-binding PKC substrate	Increase	2.7
Diacylglycerol kinase (Ca^{2+} stimulated)	Decrease	2.6

PKC, protein kinase C; ALDO, aldosterone.

Table 3. *Differentially expressed genes associated with oxidative stress and immune stimulation in ALDOST compared with unoperated and untreated controls*

Gene Product	Effects of ALDO, fold change
Oxidative stress and antioxidant reserves	
Mn^{2+}-superoxide dismutase	+2.2
Glutathione reductase	+3.3
NADPH oxidoreductase	+3.6
Inducible nitric oxide synthase	+4.7
Inflammation	
Intercellular adhesion molecule-1	+2.1
CC chemokine receptor protein	+2.9
Chemokine receptor CCR2	+3.8
CXC chemokine receptor	+2.6
Interleukin-1β	+8.6
Interleukin-1β receptor type 2	+2.4
5-Lipoxygenase activating protein	+3.6
Substance P receptor	+2.1
Lymphocyte activation	
IgG1-γ heavy chain (M28670)	+12.8
IgA constant region	+7.2
IgE binding protein	+4.2
Anti-acetylcholine receptor antibody	+7.0
RT6 (depleted in autoimmunity)	−4.8

argy, elevated blood pressure, or immunohistochemical evidence of cardiac pathology at *week 4*. Values for $[Mg^{2+}]_i$ observed in PBMCs at *week 1* ALDOST were significantly reduced compared with age- and gender-matched UO and UN controls. Our control values conform with those reported by others for lymphocytes obtained from rodents on a normal diet (59). Factors that could have contributed to this decrease in $[Mg^{2+}]_i$ were considered. We did not monitor urinary or fecal Mg^{2+} excretion in our rats that received ALDOST; both are increased in patients with PAL and in adrenalectomized rats treated with ALDO (28, 30) and can ultimately lead to hypomagnesemia, which has been reported in several patients with long-standing adrenal adenoma and where normal Mg^{2+} homeostasis is restored following surgical removal of the adrenal tumor (30, 36, 43). In the present study, plasma Mg^{2+} levels at 1 and 4 wks of ALDOST remained within the normal range and were statistically indistinguishable from our two control groups. Dietary Mg^{2+} deficiency can lead to reduced Mg^{2+} levels in PBMCs (58, 70, 71). The Mg^{2+} content of the standard dietary feed we used is 20–40 mmol/kg in keeping with daily rodent requirements and is quite unlike the diets that are used to induce Mg^{2+} deficiency (which have <2 mmol/kg Mg^{2+}; Refs. 70, 71). We therefore conclude that dietary deficiency was not involved in the observed reduction in PBMC $[Mg^{2+}]_i$. Lymphocytes have ALDO receptors (2), and Delva et al. (20) found a Na^+-dependent decline in cultured human lymphocyte $[Mg^{2+}]_i$ that reached a maximum within 120 min when these cells were incubated with ALDO in physiological concentrations. Na^+/Mg^{2+} exchange sites that may be operative in this response are illustrated in Fig. 5 (56). This efflux of $[Mg^{2+}]_i$ is abrogated by blocking the receptor-ligand

binding with canrenoic acid and also by inhibiting transcription and protein synthesis with actinomycin D and cycloheximide, respectively (20). These investigators also observed a reduction in lymphocyte $[Mg^{2+}]_i$ in patients with PAL. We therefore conclude that the reductions in PBMC $[Mg^{2+}]_i$ that we observed at *weeks 1* and *4* in our rat model of aldosteronism are related to an ALDO-mediated Na^+-dependent response that likely involves a Na^+/Mg^{2+} exchanger. Previous studies from this laboratory have shown coronary lesions do not appear when ALDO administration is combined with a diet that is deficient in NaCl or with a 1% NaCl diet without ALDO treatment in uninephrectomized controls (10). Hence, we believe that both ALDO and Na^+ are needed to drive Mg^{2+} efflux from PBMCs and initiate the pathogenic inflammatory process. Future in vivo studies that use either an ALDO receptor antagonist or an inhibitor of the Na^+/Mg^{2+} exchanger (56, 61) as cotreatment with ALDOST are planned.

A second major finding of the present study and concordant with the early reduction in $[Mg^{2+}]_i$ is the activation of the PBMC transcriptome that appears at *week 1* of ALDOST, where 205 genes were either up- or downregulated. Mg^{2+} is an important intracellular divalent cation that is involved in hundreds of enzymatic reactions, many of which are related to ATPases and GTPases. Most Mg^{2+} is inactive, bound to ATP within the cytosol and within such organelles as endoplasmic reticulum and mitochondria; its relatively small ionized fraction is biologically active. In response to the
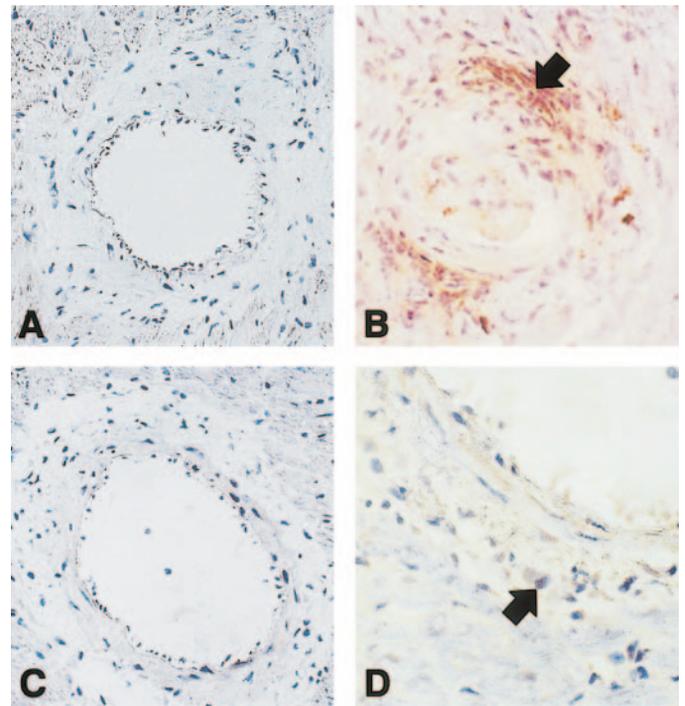

Fig. 4. In rats that received 4 wks ALDOST, expression of gp91[phox] and 3-nitrotyrosine was detected via immunolabeling and found to involve inflammatory cells (arrowheads) located in the perivascular space of intramural coronary arteries. UO controls and 4-wk ALDOST are shown for gp91[phox] (*A* and *B*, respectively) and 3-nitrotyrosine (*C* and *D*, respectively). Magnification, ×280 (*A–C*) and ×420 (*D*).

Fig. 5. Na^+/Mg^{2+} and Mg^{2+}/Ca^{2+} exchange sites and Mg^{2+}-dependent Na^+-K^+-ATPase in PBMCs. ALDO, aldosterone. [Adapted from Romani and Scarpa (56).]
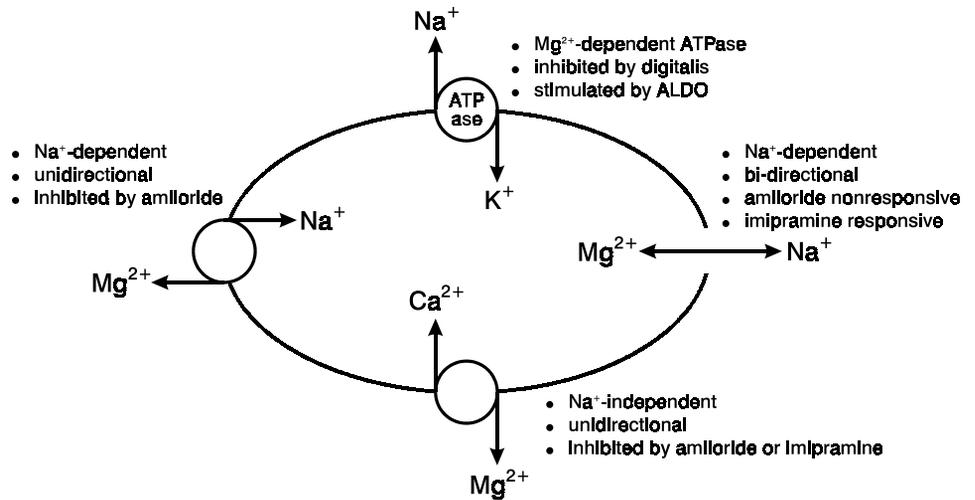
decrease in $[Mg^{2+}]_i$ that appears in PBMCs at *week 1* ALDOST, we found reduced expression of genes for the α_1-isoform of Na^+-K^+-ATPase, ATP-dependent RNA helicase, and cGMP-stimulated phosphodiesterase. Reduced tissue Na^+-K^+-ATPase activity, which is associated with a Mg^{2+}-deficient diet in rats and hamsters, is accompanied by an increase in Na^+ and Ca^{2+} concentrations in skeletal and cardiac muscle and bone and where the elevation in tissue Ca^{2+} occurs via a Na^+/Ca^{2+} exchanger (17, 35). Our data indicate that a similar process may occur in PBMCs. Another factor that could account for a reduction in Na^+-K^+-ATPase activity in our rat model is an increase in endogenous circulating ouabain, which is a Na^+-K^+-ATPase inhibitor that is known to accompany PAL and is normalized after surgical removal of adrenal adenoma (57).

A third major finding of this study was the responses in PBMC $[Ca^{2+}]_i$ and transcriptome events associated with Ca^{2+} overload. An accompaniment to reduced Na^+-K^+-ATPase activity would be an increase in Na^+ entry followed by the stoichiometric exchange of 3 Na^+ for 1 Ca^{2+} via a Na^+/Ca^{2+} exchanger (48). The influx of Ca^{2+} contributes to a Ca^{2+} overload, which initially is shunted to intracellular stores such as mitochondria where an induction of oxidative and nitrosative stress occurs (6, 23, 51, 61). We found upregulated expression of Mn^{2+}-SOD, which is specific to mitochondria-based antioxidant reserves (60). After the saturation of organelles is a subsequent increase in $[Ca^{2+}]_i$, which may be facilitated by the decline in $[Mg^{2+}]_i$, its physiological antagonist, and nitric oxide-mediated release of Ca^{2+} from mitochondrial stores (29). Our analysis of PBMC transcriptomes revealed increased expression of iNOS. Furthermore, Wehling et al. (72) found that ALDO reduces the efflux of $[Ca^{2+}]_i$ from cultured PBMCs in a Na^+-dependent manner inhibited by amiloride. Shifts in intracellular divalent cations are a key component associated with transcriptional activation of many different cell types including lymphocytes (11, 22, 54, 55, 73). We observed induction of a number of transcripts associated with defenses against free radical production, with the presence of oxidative and nitrosative

stress indicated by reduced plasma α_1-AP and immunohistochemical evidence of gp91^{phox} expression [an NADPH oxidase subunit that is specific to leukocytes and endothelial cells (60)] and the presence of 3-nitrotyrosine in PBMCs that invaded the coronary vasculature. For the PBMC transcriptomes, these included expression of antioxidant reserves such as Mn^{2+}-SOD, glutathione reductase, NADPH oxireductase, and iNOS. Each of these reserves are activated during inflammatory states (33). In humans and experimental animals, neurohormonal activation is accompanied by induction of oxidative and nitrosative stress in plasma, skeletal muscle, heart, and PMBCs (3, 16, 18, 62, 69, 74).

Finally, the early activation of specific immune responses in the PBMC transcriptomes that appeared at *week 1* of ALDOST was sustained and progressive at
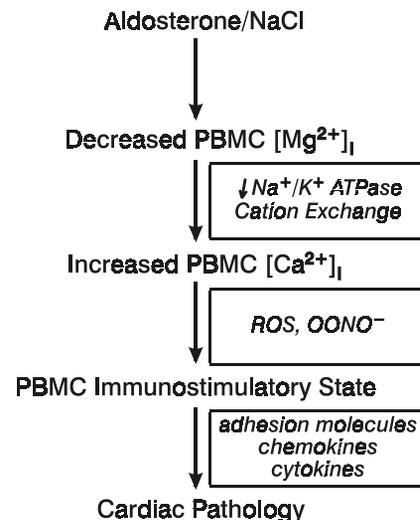
Fig. 6. A model paradigm of the immunostimulatory state that is induced in PBMCs by ALDOST and the accompanying iterations in $[Mg^{2+}]_i$ and $[Ca^{2+}]_i$ with Ca^{2+} overload that results in oxidative and nitrosative stress with reactive oxygen species (ROS) and peroxynitrite (OONO$^-$) formation. Supporting molecular evidence (indicated in boxes) is observed as shifts in transcriptomes occur during the PBMC-mediated immunostimulatory state that leads to cardiac pathology.

week 4, where 230 genes were upregulated, whereas 201 were downregulated. This included induction of inflammatory responses such as ICAM-1, chemokine receptor protein and receptor, IL-1β and its receptor, and substance P receptor. Upregulation of ICAM-1 and chemokine receptor genes can stimulate leukocyte movement and migration across the endothelium and media into the perivascular space, where we found immunohistochemical evidence of oxidative and nitrosative stress in inflammatory cells and previously have localized (by in situ hybridization) upregulated mRNA expression of ICAM-1, MCP-1, and TNF-α in these cells at sites of cardiac lesions (65). This immunostimulatory state is further accompanied by upregulation of immunoglobulins, in keeping with B lymphocyte activation, and activation of specific, perhaps autoreactive, immune responses that include upregulation of anti-acetylcholine receptor antibody expression and downregulation of RT6 gene, which is depleted in autoimmunity (76). If specific immune responses were involved in attracting activated PBMCs to the coronary vasculature, this could explain why heart tissue is not affected until *week 4* of ALDOST. Autoimmune-mediated injury could contribute to a progressive structural remodeling of the heart and impair its pump function.

Weglicki and coworkers (70, 71) presented evidence of oxidative and nitrosative stress within plasma, reduced antioxidant reserves in PBMCs, elevated PBMC proinflammatory cytokine production, and substance P receptor expression at *week 1* of a Mg^{2+}-deficient diet in rats; these effects preceded cardiac lesions that appeared at *week 3,* and a substance P receptor antagonist proved to be cardioprotective. Additional evidence linking PBMC behavior and altered immunity with Mg^{2+} deficiency in adult animals has been reported including exaggerated superoxide production and Ca^{2+}-mobilizing capacity in response to live bacteria or platelet-activating factors (38) and hyperplasia of bone marrow and thymus (4, 7, 31, 40, 41). In young weanling rats, cDNA array studies demonstrate that Mg^{2+} deficiency is accompanied by upregulation of stress protein expression in neutrophils and thymocytes; apoptosis and heat shock proteins in neutrophils (13); and cytochrome oxidase, glutathione transferase, SOD, and heat shock proteins in thymocytes (47).

Heart failure is a major health problem of epidemic proportions. Irrespective of its etiologic origins, a dysfunction of this normally efficient muscular pump during either its ejection or filling phases (i.e., systolic and diastolic dysfunction, respectively) is associated with systemic consequences that lead to a progressive downhill clinical course. Why? Neurohormonal system activation. Sustained release of effector hormones of the renin-angiotensin-ALDO system are maladapative. They not only account for salt and water retention and the congestive heart failure syndrome, they become stressors that invoke a progressive systemic illness. Featured are oxidative and nitrosative stress in PBMCs and plasma (18, 21, 32); a "cytokine storm" with elevated plasma levels of proinflammatory cytokines (44, 67, 68); and anorexia, lethargy, and tissue

wasting (1). Herein we used a rodent model to address one aspect of the neurohormonal profile of human heart failure, namely, that related to aldosteronism, which is defined as chronic elevation in plasma ALDO that is inappropriate for dietary Na^+ intake and its association with immune cell activation. During *week 1* of ALDOST (a preclinical stage), we found upregulation of the PBMC transcriptomes that featured inflammatory responses and lymphocyte activation. The triggering mechanism associated with this activation was a reduction in PBMC $[Mg^{2+}]_i$ and was accompanied by upregulation of oxidative and nitrosative stress-related genes and those representing antioxidant reserves. This immunostimulatory state preceded (by weeks) the appearance of clinical illness with lethargy and anorexia and the proinflammatory, profibrogenic cardiac phenotype with coronary vascular lesions. Moreover, autoreactive immune responses were observed that may explain the delayed nature of cardiac lesions and raise the prospect of an autoimmune-type response that could contribute to the progressive remodeling and adverse function of myocardium that is seen in humans with chronic cardiac failure. ALDO-mediated, Na^+-dependent efflux of Mg^{2+} has been observed in cultured human lymphocytes, and lymphocyte $[Mg^{2+}]_i$ is reduced in patients with PAL (20). Yndestad et al. (74) found upregulated expression of a TNF family of ligands in the transcriptome of PBMCs obtained from patients with heart failure. Our findings not only broaden the concept of an immunoneuroendocrine interface (42), but they raise the intriguing prospect that information derived from the PBMC transcriptomes (as may also be the case for their proteomes) may serve as noninvasive biomarkers of disease risk, onset, and progression in human heart failure. This remains to be elucidated.

In summary, we conducted a detailed molecular characterization of PBMCs at 1 and 4 wks in a rat model of aldosteronism. On the basis of our findings, we propose a paradigm that is depicted in Fig. 6 in which an immunostimulatory state that is already present at *week 1* (preclinical stage) precedes systemic illness and coronary vascular remodeling that appears at *week 4*. Initial shifts in divalent cation concentrations ($[Mg^{2+}]_i$ and $[Ca^{2+}]_i$) lead to oxidative and nitrosative stress and activation of PBMCs, which may then target the vasculature of intramural coronary arteries to initiate the proinflammatory, profibrogenic cardiac phenotype.

REFERENCES

1. **Anker SD, Chua TP, Ponikowski P, Harrington D, Swan JW, Kox WJ, Poole-Wilson PA, and Coats AJS.** Hormonal changes and catabolic/anabolic imbalance in chronic heart fail-

ure and their importance for cardiac cachexia. *Circulation* 96: 526–534, 1997.

2. **Armanini D, Strasser T, and Weber PC.** Characterization of aldosterone binding sites in circulating human mononuclear leukocytes. *Am J Physiol Endocrinol Metab* 248: E388–E390, 1985.

3. **Ball AM and Sole MJ.** Oxidative stress and the pathogenesis of heart failure. *Cardiol Clin* 16: 665–675, 1998.

4. **Battifora HA, McCreary PA, Hahneman BM, Laing GH, and Hass GM.** Chronic magnesium deficiency in the rat. Studies of chronic myelogenous leukemia. *Arch Pathol* 86: 610–620, 1968.

5. **Bhattacharya SK.** Simultaneous determination of calcium and magnesium in human blood serum by atomic absorption spectrophotometer. *Anal Lett* 10: 817–830, 1977.

6. **Bhattacharya SK, Johnson PL, and Thakar JH.** Reversal of impaired oxidative phosphorylation and calcium overloading in the skeletal muscle mitochondria of CHF-146 dystrophic hamsters. *Mol Chem Neuropathol* 34: 53–77, 1998.

7. **Bois P.** Tumour of the thymus in magnesium-deficient rats. *Nature* 204: 1316, 1964.

8. **Boudier C and Bieth JG.** Oxidized mucus proteinase inhibitor: a fairly potent neutrophil elastase inhibitor. *Biochem J* 303: 61–68, 1994.

9. **Brilla CG, Pick R, Tan LB, Janicki JS, and Weber KT.** Remodeling of the rat right and left ventricle in experimental hypertension. *Circ Res* 67: 1355–1364, 1990.

10. **Brilla CG and Weber KT.** Mineralocorticoid excess, dietary sodium and myocardial fibrosis. *J Lab Clin Med* 120: 893–901, 1992.

11. **Brown KC and Kodadek T.** Protein cross-linking mediated by metal ion complexes. *Met Ions Biol Syst* 38: 351–384, 2001.

12. **Burritt JB, Quinn MT, Jutila MA, Bond CW, and Jesaitis AJ.** Topological mapping of neutrophil cytochrome b epitopes with phage-display libraries. *J Biol Chem* 270: 16974–16980, 1995.

13. **Bussière FI, Zimowska W, Gueux E, Rayssiguier Y, and Mazur A.** Stress protein expression cDNA array study supports activation of neutrophils during acute magnesium deficiency in rats. *Magnes Res* 15: 37–42, 2002.

14. **Campbell SE, Diaz-Arias AA, and Weber KT.** Fibrosis of the human heart and systemic organs in adrenal adenoma. *Blood Press* 1: 149–156, 1992.

15. **Campbell SE, Janicki JS, and Weber KT.** Temporal differences in fibroblast proliferation and phenotype expression in response to chronic administration of angiotensin II or aldosterone. *J Mol Cell Cardiol* 27: 1545–1560, 1995.

16. **Cesselli D, Jakoniuk I, Barlucchi L, Beltrami AP, Hintze TH, Nadal-Ginard B, Kajstura J, Leri A, and Anversa P.** Oxidative stress-mediated cardiac cell death is a major determinant of ventricular dysfunction and failure in dog dilated cardiomyopathy. *Circ Res* 89: 279–286, 2001.

17. **Chang C and Bloom S.** Interrelationship of dietary Mg intake and electrolyte homeostasis in hamsters. I. Severe Mg deficiency, electrolyte homeostasis, and myocardial necrosis. *J Am Coll Nutr* 4: 173–185, 1985.

18. **Chen L, Zang Y, Bai B, Zhu M, Zhao B, Hou J, and Xin W.** Electron spin resonance determination and superoxide dismutase activity in polymorphonuclear leukocytes in congestive heart failure. *Can J Cardiol* 8: 756–760, 1992.

19. **Cho Y, Jang YY, Han ES, and Lee CS.** The inhibitory effect of ambroxol on hypochlorous acid-induced tissue damage and respiratory burst of phagocytic cells. *Eur J Pharmacol* 383: 83–91, 1999.

20. **Delva P, Pastori C, Degan M, Montesi G, Brazzarola P, and Lechi A.** Intralymphocyte free magnesium in patients with primary aldosteronism: aldosterone and lymphocyte magnesium homeostasis. *Hypertension* 35: 113–117, 2000.

21. **Diaz-Velez CR, Garcia-Castineiras S, Mendoza-Ramos E, and Hernandez-Lopez E.** Increased malondialdehyde in peripheral blood of patients with congestive heart failure. *Am Heart J* 131: 146–152, 1996.

22. **Di Francesco A, Desnoyer RW, Covacci V, Wolf FI, Romani A, Cittadini A, and Bond M.** Changes in magnesium content

and subcellular distribution during retinoic acid-induced differentiation of HL60 cells. *Arch Biochem Biophys* 360: 149–157, 1998.

23. **Duchen MR.** Contributions of mitochondria to animal physiology: from homeostatic sensor to calcium signalling and cell death. *J Physiol* 516: 1–17, 1999.

24. **Everett AD, Tufro-McReddie A, Fisher A, and Gomez RA.** Angiotensin receptor regulates cardiac hypertrophy and transforming growth factor-α1 expression. *Hypertension* 23: 587–592, 1994.

25. **Fontana M, Pecci L, Macone A, and Cavallini D.** Antioxidant properties of the decarboxylated dimer of aminoethylcysteine ketimine: assessment of its ability to scavenge peroxynitrite. *Free Radic Res* 29: 435–440, 1998.

26. **Grynkiewicz G, Poenie M, and Tsien RY.** A new generation of Ca^{2+} indicators with greatly improved fluorescence properties. *J Biol Chem* 260: 3440–3450, 1985.

27. **Hall CE and Hall O.** Hypertension and hypersalimentation. I. Aldosterone hypertension. *Lab Invest* 14: 285–294, 1965.

28. **Hanna S and MacIntyre I.** The influence of aldosterone on magnesium metabolism. *Lancet* 2: 348–350, 1960.

29. **Horn TF, Wolf G, Duffy S, Weiss S, Keilhoff G, and MacVicar BA.** Nitric oxide promotes intracellular calcium release from mitochondria in striatal neurons. *FASEB J* 16: 1611–1622, 2002.

30. **Horton R and Biglieri EG.** Effect of aldosterone on the metabolism of magnesium. *J Clin Endocrinol Metab* 22: 1187–1192, 1962.

31. **Jasmin G.** LymphŒdème, hyperplasie et tuméfaction du tissu lymphatique chez le rat soumis à une diète déficiente en magnésium. *Rev Can Biol* 22: 383–390, 1963.

32. **Keith M, Geranmayegan A, Sole MJ, Kurian R, Robinson A, Omran AS, and Jeejeebhoy KN.** Increased oxidative stress in patients with congestive heart failure. *J Am Coll Cardiol* 31: 1352–1356, 1998.

33. **Loscalzo J.** Inducible NO synthesis in the vasculature: molecular context defines physiological response. *Arterioscler Thromb Vasc Biol* 21: 1259–1260, 2001.

34. **Loscalzo J.** Salt-sensitive hypertension and inducible nitric oxide synthase: form-function dichotomy of a coding region mutation, Mutatis mutandis. *Circ Res* 89: 292–294, 2001.

35. **Madden JA, Smith GA, and Llaurado JG.** Myocardial K kinetics in rats on Mg-deficient diet. *J Am Coll Nutr* 1: 323–329, 1982.

36. **Mader IJ and Iseri LT.** Spontaneous hypopotassemia, hypomagnesemia, alkalosis and tetany due to hypersecretion of corticosterone-like mineralocorticoid. *Am J Med* 19: 976–988, 1955.

37. **Mak IT, Komarov AM, Wagner TL, Stafford RE, Dickens BF, and Weglicki WB.** Enhanced NO production during Mg deficiency and its role in mediating red blood cell glutathione loss. *Am J Physiol Cell Physiol* 271: C385–C390, 1996.

38. **Malpuech-Brugere C, Rock E, Astier C, Nowacki W, Mazur A, and Rayssiguier Y.** Exacerbated immune stress response during experimental magnesium deficiency results from abnormal cell calcium homeostasis. *Life Sci* 63: 1815–1822, 1998.

39. **Martinez DV, Rocha R, Matsumura M, Oestreicher E, Ochoa-Maya M, Roubsanthisuk W, Williams GH, and Adler GK.** Cardiac damage prevention by eplerenone: comparison with low sodium diet or potassium loading. *Hypertension* 39: 614–618, 2002.

40. **McCreary PA, Battifora HA, Hahneman BM, Laing GH, and Hass GM.** Leukocytosis, bone marrow hyperplasia and leukemia in chronic magnesium deficiency in the rat. *Blood* 29: 683–690, 1967.

41. **McCreary PA, Battifora HA, Laing GH, and Hass GM.** Protective effect of magnesium deficiency on experimental allergic encephalomyelitis in the rat. *Proc Soc Exp Biol Med* 121: 1130–1133, 1966.

42. **Melmed S.** Series introduction. The immuno-neuroendocrine interface. *J Clin Invest* 108: 1563–1566, 2001.

43. **Milne MD, Muehrcke RC, and Aird I.** Primary aldosteronism. *QJM* 26: 317–335, 1957.

44. **Munger MA, Johnson B, Amber IJ, Callahan KS, and Gilbert EM.** Circulating concentrations of proinflammatory cyto-

kines in mild or moderate heart failure secondary to ischemic or idiopathic dilated cardiomyopathy. *Am J Cardiol* 77: 723–727, 1996.

45. **Nicoletti A, Mandet C, Challah M, Bariety J, and Michel JB.** Mediators of perivascular inflammation in the left ventricle of renovascular hypertensive rats. *Cardiovasc Res* 31: 585–595, 1996.

46. **Paolo G, Paola G, Baena Y, Riccardo R, Catherine K, Vittorio G, Fulvio T, Barbara B, Flavio T, Nicoletta F, and Fulvio M.** Inactivation of alpha1-antiproteinase (alpha1-AT) and changes in antioxidants' plasma levels in subarachnoid hemorrhage. *J Neurol Sci* 152: 154–159, 1997.

47. **Petrault I, Zimowska W, Mathieu J, Bayle D, Rock E, Favier A, Rayssiguier Y, and Mazur A.** Changes in gene expression in rat thymocytes identified by cDNA array support the occurrence of oxidative stress in early magnesium deficiency. *Biochim Biophys Acta* 1586: 92–98, 2002.

48. **Philipson KD and Nicoll DA.** Sodium-calcium exchange: a molecular perspective. *Annu Rev Physiol* 62: 111–133, 2000.

49. **Raju B, Murphy E, Levy LA, Hall RD, and London RE.** A fluorescent indicator for measuring cytosolic free magnesium. *Am J Physiol Cell Physiol* 256: C540–C548, 1989.

50. **Rijkers GT, Henriquez N, and Griffioen AW.** Intracellular magnesium movements and lymphocyte activation. *Magnes Res* 6: 205–213, 1993.

51. **Rizzuto R, Bernardi P, and Pozzan T.** Mitochondria as all-round players of the calcium game. *J Physiol* 529: 37–47, 2000.

52. **Robert V, Van Thiem N, Cheav SL, Mouas C, Swynghedauw B, and Delcayre C.** Increased cardiac types I and III collagen mRNAs in aldosterone-salt hypertension. *Hypertension* 24: 30–36, 1994.

53. **Rocha R, Stier CT Jr, Kifor I, Ochoa-Maya MR, Rennke HG, Williams GH, and Adler GK.** Aldosterone: a mediator of myocardial necrosis and renal arteriopathy. *Endocrinology* 141: 3871–3878, 2000.

54. **Rodrigues-Lima F, Josephs M, Katan M, and Cassinat B.** Sequence analysis identifies TTRAP, a protein that associates with CD40 and TNF receptor-associated factors, as a member of a superfamily of divalent cation-dependent phosphodiesterases. *Biochim Biophys Res Commun* 285: 1274–1279, 2001.

55. **Romani A and Scarpa A.** Regulation of cell magnesium. *Arch Biochem Biophys* 298: 1–12, 1992.

56. **Romani AM and Scarpa A.** Regulation of cellular magnesium. *Front Biosci* 5: D720–D734, 2000.

57. **Rossi G, Manunta P, Hamlyn JM, Pavan E, De Toni R, Semplicini A, and Pessina AC.** Immunoreactive endogenous ouabain in primary aldosteronism and essential hypertension: relationship with plasma renin, aldosterone and blood pressure levels. *J Hypertens* 13: 1181–1191, 1995.

58. **Ryan MF and Ryan MP.** Lymphocyte electrolyte alterations during magnesium deficiency in the rat. *Ir J Med Sci* 148: 108–109, 1979.

59. **Sasaki N, Oshima T, Matsuura H, Yoshimura M, Yashiki M, Higashi Y, Ishioka N, Nakano Y, Kojima R, Kambe M, and Kajiyama G.** Lack of effect of transmembrane gradient of magnesium and sodium on regulation of cytosolic free magnesium concentration in rat lymphocytes. *Biochim Biophys Acta* 1329: 169–173, 1997.

60. **Schumacker PT.** Angiotensin II signaling in the brain: compartmentalization of redox signaling? *Circ Res* 91: 982–984, 2002.

61. **Simchowitz L, Foy MA, and Cragoe EJ Jr.** A role for Na^+/Ca^{2+} exchange in the generation of superoxide radicals by human neutrophils. *J Biol Chem* 265: 13449–13456, 1990.

62. **Singal PK, Beamish RE, and Dhalla NS.** Potential oxidative pathways of catecholamines in the formation of lipid peroxides and genesis of heart disease. *Adv Exp Med Biol* 161: 391–401, 1983.

63. **Sun Y, Ramires FJA, and Weber KT.** Fibrosis of atria and great vessels in response to angiotensin II or aldosterone infusion. *Cardiovasc Res* 35: 138–147, 1997.

64. **Sun Y and Weber KT.** Angiotensin II and aldosterone receptor binding in rat heart and kidney: response to chronic angiotensin II or aldosterone administration. *J Lab Clin Med* 122: 404–411, 1993.

65. **Sun Y, Zhang J, Lu L, Chen SS, Quinn MT, and Weber KT.** Aldosterone-induced inflammation in the rat heart. Role of oxidative stress. *Am J Pathol* 161: 1773–1781, 2002.

66. **Sun Y, Zhang J, Zhang JQ, and Ramires FJA.** Local angiotensin II and transforming growth factor-beta1 in renal fibrosis of rats. *Hypertension* 35: 1078–1084, 2000.

67. **Testa M, Yeh M, Lee P, Fanelli R, Loperfido F, Berman JW, and LeJemtel TH.** Circulating levels of cytokines and their endogenous modulators in patients with mild to severe congestive heart failure due to coronary artery disease or hypertension. *J Am Coll Cardiol* 28: 964–971, 1996.

68. **Torre-Amione G, Kapadia S, Benedict C, Oral H, Young JB, and Mann DL.** Proinflammatory cytokine levels in patients with depressed left ventricular ejection fraction: a report from the Studies of Left Ventricular Dysfunction (SOLVD). *J Am Coll Cardiol* 27: 1201–1206, 1996.

69. **Tsutsui H, Ide T, Hayashidani S, Suematsu N, Shiomi T, Wen J, Nakamura K, Ichikawa K, Utsumi H, and Takeshita A.** Enhanced generation of reactive oxygen species in the limb skeletal muscles from a murine infarct model of heart failure. *Circulation* 104: 134–136, 2001.

70. **Weglicki WB, Mak IT, and Phillips TM.** Blockade of cardiac inflammation in Mg^{2+} deficiency by substance P receptor inhibition. *Circ Res* 74: 1009–1013, 1994.

71. **Weglicki WB, Mak IT, Stafford RE, Dickens BF, Cassidy MM, and Phillips TM.** Neurogenic peptides and the cardiomyopathy of magnesium-deficiency: effects of substance P-receptor inhibition. *Mol Cell Biochem* 130: 103–109, 1994.

72. **Wehling M, Käsmayr J, and Theisen K.** Aldosterone influences free intracellular calcium in human mononuclear leukocytes in vitro. *Cell Calcium* 11: 565–571, 1990.

73. **Wolf FI, Covacci V, Bruzzese N, Di Francesco A, Sacchetti A, Corda D, and Cittadini A.** Differentiation of HL-60 promyelocytic leukemia cells is accompanied by a modification of magnesium homeostasis. *J Cell Biochem* 71: 441–448, 1998.

74. **Yndestad A, Damås JK, Eiken HG, Holm T, Haug T, Simonsen S, Frøland SS, Gullestad L, and Aukrust P.** Increased gene expression of tumor necrosis factor superfamily ligands in peripheral blood mononuclear cells during chronic heart failure. *Cardiovasc Res* 54: 175–182, 2002.

75. **Young M, Head G, and Funder J.** Determinants of cardiac fibrosis in experimental hypermineralocorticoid states. *Am J Physiol Endocrinol Metab* 269: E657–E662, 1995.

76. **Zinkernagel RM.** On differences between immunity and immunological memory. *Curr Opin Immunol* 14: 523–536, 2002.